THz-Micro-Spectroscopy

Bruno Gompf and Martin Dressel

***Abstract*—We compare different near-field methods operating in the frequency range between 50 GHz and 1.5 THz with respect to their application potential for terahertz-micro-spectroscopy. Scanning near-field optical microscopes (SNOMs) can be divided into two basic principles: aperture SNOMs using a small pinhole and apertureless SNOMs, where a small scatterer acts as a near-field probe. As an alternative method, we include in our comparison a microscope based on a solid immersion lens. Most of these techniques are well known in the visible and infrared range, where they are mainly utilized to reach a high spatial resolution. In real samples, the physics behind the observed image contrast is often unclear, and therefore, additional spectroscopic information on a subwavelength spot size is desired. In this paper, we discuss different microscopic techniques in respect of their micro-spectroscopic potential in the THz range.**

***Index Terms*—Aperture scanning near-field optical microscopes (SNOM), near-field imaging, submillimeter spectroscopy, terahretz (THz) image contrast, THz spectroscopy.**

I. Introduction

BESIDES the lack of cheap and easy-to-use sources and detectors, a broader application of terahertz (THz)-radiation in material sciences, biology, and medicine is hampered by the very long wavelength of this radiation (0.1–3 mm), which strongly limits the spatial resolution of microscopic methods in the far field. Not only the samples in life sciences, for example, are inherently inhomogeneous on a length scale of micrometers, but in physics and material science also, one often have to deal with structures or crystals much smaller than the wavelength in the THz-range. In principle, with scanning near-field microscopes (SNOMs), this limitation can be overcome, and great progress has been achieved over the last two decades, especially in the visible region [1]. Also in the regime of radio frequencies through far-infrared, enormous efforts were devoted to improve the spatial resolution. Rosner and van der Weide [2] recently gave a good overview on near-field methods in this frequency range. Nevertheless, until now, near-field techniques have been mainly used to obtain spatial information and not to perform quantitative spectroscopy.

SNOMs can roughly be divided into two principles: aperture SNOMs in which a small pinhole acts as a subwavelength source or detector and apertureless SNOMs where a small scatterer is used as a near-field probe. In both the techniques, the trade-off for the enhanced resolution is a very low signal. However, real samples normally exhibit only small differences in their overall optical properties, but that is the relevant information. Therefore, it would be desirable to have the choice between higher resolution and higher dynamic range. To demonstrate that a resolution enhancement is also possible without loosing intensity, we include the solid immersion lens (SIL) microscopy in our comparison.

The main aim of this paper is to summarize and compare the different approaches with regard to their potential for micro-spectroscopic applications. At THz frequencies, the observed image contrast is often not clear, mainly due to the fact that the underlying absorption process is unknown; hence, additional spectroscopic information is highly desired.

Manuscript received September 1, 2007; revised September 5, 2007. This work was supported in part by the Deutsche Forschungsgemeinschaft (DFG) under Grant Dr228/24-2 and in part by the Landesstiftung Baden-Württemberg in the framework of "Forschung Optische Technologien."

The authors are with the Physikalisches Institut, Universität Stuttgart, 70550 Stuttgart, Germany (e-mail: gompf@pi1.physik.uni-stuttgart.de; dressel@pi1.physik.uni-stuttgart.de).

Color versions of one or more of the figures in this paper are available online at http://ieeexplore.ieee.org.

Digital Object Identifier 10.1109/JSTQE.2007.910560

II. Backward-Wave Oscillators

Since we are mainly interested in spectroscopy on subwavelength spot sizes, we need widely tunable sources for our investigations. The least investigated part of the THz spectrum, and therefore, the most interesting is the range between 100 GHz and 1 THz. Below this frequency region, electronic devices such as network analyzers are available, which have high output power and can be tuned over a more or less broad frequency range. Above 1 THz, commercial FTIR-spectrometers are established and work quite well. They also cover a very broad spectral range in combination with a high spectral resolution. Beside large facility sources, like synchrotrons and free electron lasers, there is only one table-top source available that fulfills all the required specifications for near-field spectroscopy, i.e., combines high spectral resolution with a broad frequency range in the aforementioned THz regime: backward-wave oscillators (BWO). Most other sources either did not work in the aforementioned frequency range (quantum cascade laser [5], Ge-laser [6]), are not tunable over a broader range (gas laser), or have only very limited output power, such as all techniques generating THz radiation by a nonlinear process, for example, the time-domain techniques [3]. For micro-spectroscopy, the time-domain techniques have the additional problem that small apertures always act as high-pass filters for broadband radiation [4].

BWOs supply highly monochromatic $(\Delta\nu/\nu \approx 10^{-6})$ and coherent radiation with an output power of up to 100 mW [7]. Each BWO can be tuned over a frequency range of about a factor of 2, so that a dozen sources span the spectral range from 30 GHz to 1.4 THz (corresponding to $1-50\ \mathrm{cm}^{-1}$).

III. Solid-Immersion-Lens Microscopy

Although in the visible, the development of solid-immersion lens techniques has dramatically increased the capacity of optical memories [8], in the THz range, there exist only a very limited number of studies [9], [10]. Due to ionic

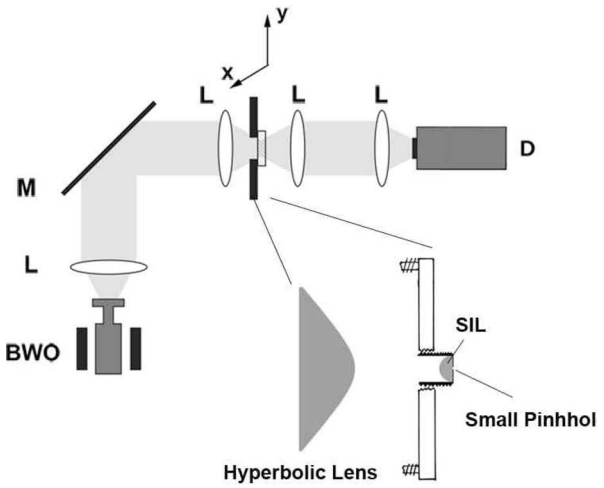

Fig. 1. Scheme of the solid immersion lens microscope. BWO, backward-wave oscillator as radiation source; L, polyethylene lenses; M, mirror; D, Golay cell as detector; SIL, solid immersion lens.

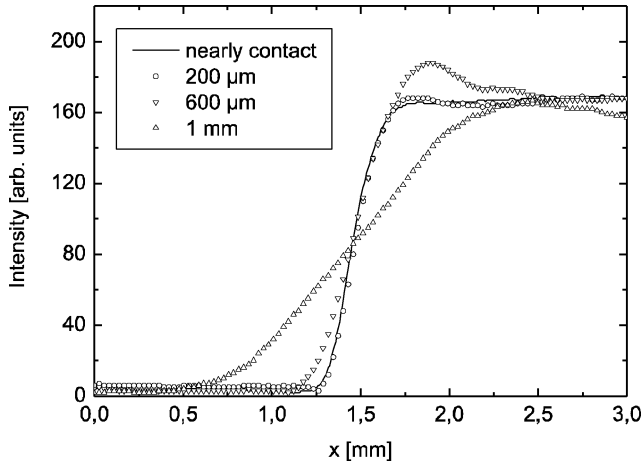

Fig. 2. Resolution tested at a sharp edge taken at different distances from the SIL. Up to a distance of the order of the wavelength, there is nearly no decrease in resolution which makes the SIL technique very insensitive to the probe-sample distance and thereby to topographic artifacts.

polarization, the refractive index of most materials is much higher at THz-frequencies than in the visible. Hence, in the THz range, refractive-index values n of up to 10 are possible, leading to a significant reduction of the wavelength. SIL imaging is really not a near-field technique but has several advantages compared to normal near-field methods. With SILs, enhanced resolution is possible without a big loss of intensity and the probe-sample distance can be much larger than that in near-field setups operating with evanescent waves.

In Fig. 1, the schematic setup of a microspectrometer based on an SIL is sketched. The THz-radiation emitted by the BWO is collimated by a plan/convex polyethylene (PE) lens to a parallel beam and afterwards focused by a hyperbolic lens to a diffraction-limited spot on the microscope stage. Hyperbolic lenses have the advantage that they produce, comparable to mirrors, aberration-free foci, and allow for much higher numerical apertures. The heart of the microscope stage consists of a hemispherical silicon SIL $(n = 3.5)$ with 8 mm diameter glued onto a thin (80 μm) copper foil with a small pinhole in the diameter of the reduced wavelength (λ/n). The sample is scanned in vicinity to the pinhole and the transmitted intensity is then focused on the detector by another set of plan/convex PE lenses. As detector, a Golay-cell, which is not extremely sensitive, is utilized, but it exhibits a flat response curve and operates at ambient conditions.

To test the resolution enhancement of the SIL setup, a sharp edge was scanned in close contact to the SIL at a frequency of 470 GHz corresponding to a wavelength of 640 μm (black line in Fig. 2). This result is compared with the resolution achieved in the far field of the hyperbolic lens. In the regular far field, we got a 10–90% rise of about 1.3 mm at this wavelength, which is close to the Gaussian spot for a beam with 23 mm diameter, focused by a lens with a focal length of 20 mm. In the vicinity of the SIL, we were able to obtain a resolution of 310 μm, which matches nicely with the expected enhancement for a SIL with $n = 3.5$.

Fig. 3. THz-SIL image $(4\ \mathrm{cm} \times 4\ \mathrm{cm})$ of an antitheft device recorded at 470 GHz. The image is made through the plastic cover protecting the electronic circuit.

Additionally, we test the sensitivity of the SIL resolution on the probe-sample separation for different distances from the SIL (Fig. 2). Up to the order of the wavelength, there is no dramatic influence on the observable resolution, which makes this technique extremely insensitive to topographic artifacts. These artifacts due to the feedback loop of the probe-sample distance control are a serious problem in most near-field techniques.

In Fig. 3, the THz-SIL image of an antitheft device recorded at 470 GHz is displayed. The picture was taken with the SIL in close contact with the opaque plastic cover protecting the electronic device. The shown structure is, therefore, not visible with bare eyes. The metal stripes with a width of 700 μm and also the 300 μm small spacing between them are clearly resolved. The recording time for the image was approximately 30 min and is mainly limited by the slow response of the Golay-cell. The SNR is better than 10^4. With a helium-cooled bolometer,

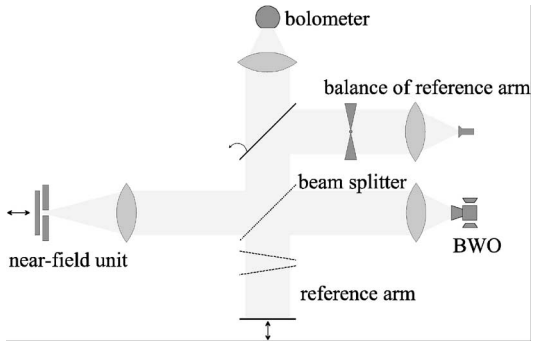

Fig. 4. Scheme of the THz-near-field spectrometer. The entire spectrometer is arranged as an interferometer to filter out the small signal absorbed by the sample from the background of high intensity reflected off the pinhole.

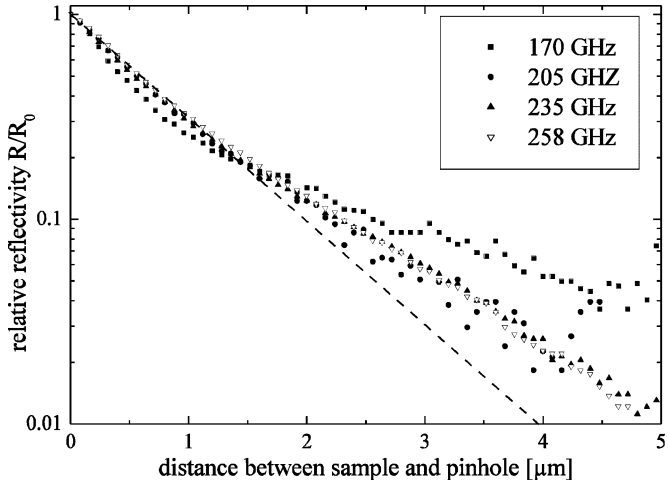

Fig. 5. Dependence of the near-field signal on the sample-pinhole distance recorded for several frequencies. The dotted line represents an exponential fit to the data.

one can gain about one order of magnitude in recording time and two orders of magnitude by the SNR. No additional sample preparation and no distance control were necessary to record the image.

IV. Aperture SNOM

Since the first demonstration of the subwavelength resolution in the microwave range by Ash and Nicholls [11], a lot of work has been invested to demonstrate that the field behind a small aperture is confined to the diameter of this aperture independent of the wavelength used. However, for another important prediction coming out of the Bethe/Bouwkamp model [12], [13] (how exactly the field intensity decreases as a function of distance from the aperture), until recently, no experimental prove exists. In fact, for aperture-based near-field spectroscopy, it is crucial that the decay of the evanescent field behind an aperture is also frequency independent.

A THz-near-field reflection spectrometer capable of investigating the spectral behavior of the evanescent field behind a subwavelength pinhole is shown in Fig. 4 [14]. Again, the radiation is generated by the BWOs and is focused onto the near-field unit that consists of two main parts: the aperture and the sample holder. As an aperture, we use pinholes of diameters down to 100 μm in thin copper foils with a thickness of 10 μm. The sample is placed in the evanescent field closely behind the pinhole. The sample can be moved relative to the aperture by three linear piezomotors. To distinguish the very low fraction absorbed by the sample from the high intensity reflected off the surrounding pinhole, two methods are employed in the setup. 1) The whole spectrometer is built as an interferometer, so that the intensity reflected off the near-field unit is balanced by a reference arm, and therefore, the detector sees nearly no intensity without sample in place. 2) The sample–pinhole distance is modulated by an additional piezo-bender. Using the lock-in technique, it can be shown that the spectrometer is only sensitive to the modulated part of the reflected signal, which is directly proportional to the absorption of the sample within the evanescent field. The distance between the pinhole and sample is controlled by a confocal microscope, not shown in Fig. 4.

For an ideally conducting and infinitely thin pinhole, the evanescent field behind the aperture should decay as

$$I(z) \propto \exp\left\{-\frac{z}{ta}\right\}$$

where z is the distance between the pinhole and the sample, a is the aperture radius and $t \approx 1.1$ is a numerical factor. This relation should hold as long as the wavelength λ is large as compared to z and a. An experimental test of this prediction is presented in Fig. 5. The measurement shows the distance-dependent decay of the near-field signal R behind a 200 μm pinhole relative to the signal at zero distance R_0. The data clearly show the same exponential decay of the near-field signal with an increasing probe–sample distance for different frequencies. At larger distances, the constant background noise together with the lower signal leads to larger deviations. As predicted by theory, the data exhibit a frequency-independent decay of the signal, but a fit to the experimental points leads to a parameter t of about 0.004, which is much smaller than the theoretical calculations. This can partly be explained by the fact that real pinholes are neither perfectly conducting nor infinitely thin. In our case, the aspect ratio (thickness/diameter) was about 0.05. Roberts, for instance, calculated for an ideal conducting pinhole with a finite thickness a much faster decay of the near-field [15]. The finite conductivity, however, prohibits the use of thinner pinholes with smaller aspect ratios. The copper used here, for example, has a specific resistivity in the frequency range of $1.7\ \mu\Omega \cdot \mathrm{cm}$ [16]. The electric field decays to $1/e$ of the original value on a length scale called the skin depth δ, which is proportional to the square root of the resistivity and the wavelength λ. For the copper, the skin depth in the frequency range between 30 GHz and 1.5 THz is 380–60 nm. Depending on the pinhole diameter and the spot size, the ratio of the radiation that shines through the hole to the total intensity is of the order of 10^{-6} to 10^{-8}. This is approximately the transmission through a solid copper foil with a thickness 13–18 times the skin depth. Thus, for near-field

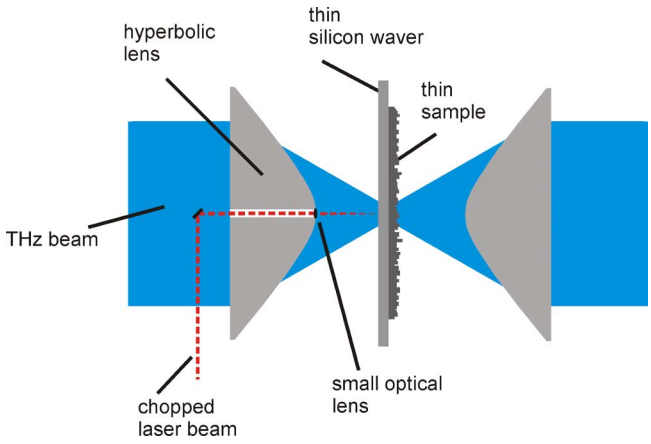

Fig. 6. Scheme of the scattering-type SNOM with photoinduced dynamic aperture. A laser beam is superimposed to the THz beam, and both beams are focused at the same spot on a thin Si wafer. At the wafer, the laser creates free charge carriers that are opaque for THz radiation. This micrometer-sized opaque region acts as an effective scatterer for the THz radiation. Using a lock-in technique the resolution achievable in the visible can thus be transferred to the THz range.

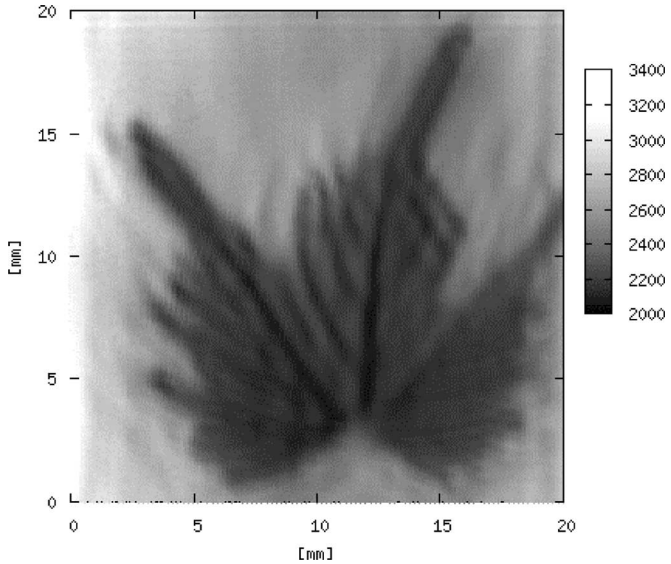

Fig. 7. THz near-field image of a freshly cut vine leaf recorded at 220 GHz corresponding to $\lambda = 1.4\,\mathrm{mm}$.

spectroscopy in the THz range, the metal foil with the pinhole cannot be much thinner than about 10 μm.

The strong but frequency-independent decay of the evanescent field has two important consequences. 1) Spectroscopy is possible with aperture-based SNOMs, but only in combination with an accurate probe–sample distance control. 2) A small modulation of this distance in combination with the lock-in technique makes it possible to measure the frequency-dependent absorption directly even for rough surfaces that show strong scattering.

V. Apertureless SNOM

In apertureless or scattering-type SNOMs (s-SNOMs), commonly the tip of an atomic force microscope is used as a small scatterer. With atomic force microscope (AFM)-based s-SNOMs, a resolution down to 150 nm has been demonstrated at 2 THz on metal-dielectric test samples [17]. The disadvantage of this method is that it mainly images the sample surface, which in most practical cases, however, is not the relevant physical information. A photoinduced dynamic aperture [18] can overcome this problem [19]. The concept is also an s-SNOM, but here the size of the scatterer is freely adjustable by optics and it also works in transmission, and therefore, images bulk properties.

A scheme of a THz near-field spectrometer based on a photoinduced aperture as near-field probe is sketched in Fig. 6 [20]. The radiation from a BWO is collimated to a parallel beam and afterwards focused to a diffraction-limited spot by a hyperbolic lens with a focal length of 20 mm. Through the center of this lens, a 5 mm hole is drilled, in which a small optical lens is glued with the same focal length. With a small mirror a green laser beam is superimposed to the THz beam so that both beams are focused on the same spot on a 150-μm-thick Si wafer. But whereas the THz beam is focused down to about 1 mm, the laser beam can be focused down to 35 μm. Normally, Si is totally transparent for THz radiation, but where it is illuminated by the laser, it becomes opaque due to the formation of free charge carriers. This micrometer-sized opaque region now acts as an effective scatterer for THz-radiation. Chopping the laser beam and using the lock-in technique for the detection allows us to obtain information only from this area. In this way, the resolution achievable in the visible can be transferred to the THz range. As long as the thickness of the Si wafer is small compared to the used THz wavelength, a sample glued at the backside of the wafer is in the near-field of the created scatterer, and can therefore, be imaged with a resolution comparable to the size of the scatterer.

In the following, we give two examples to demonstrate the importance of additional spectroscopic information for the interpretation of the observed image contrast. In Fig. 7 the THz-near-field image of a freshly cut vine leaf recorded at 220 GHz is presented. In the shown image, structures down to about 100 μm can be seen corresponding to $\lambda/14$. As mentioned before, the achievable resolution depends on the size of the opaque region created by the laser and not on the THz wavelength. However, due to the diffusion length of the photoinduced free charge carriers, this opaque region is significantly larger than the bare laser spot size. For our n-doped Si with a donor density of $10^{-16}\ \mathrm{cm}^{-3}$, the carrier lifetime is several hundred nanoseconds and the room-temperature diffusion length is about 150 μm in reasonable agreement with our results. Higher doped Si-wafers have shorter carrier lifetimes and a smaller diffusion length, and would therefore afford a better resolution. But higher doped wafers also have a lower resistivity connected with a higher absorption in the THz range and a shorter carrier lifetime, which requires a higher laser power to create a sufficient opacity.

The standard interpretation of the image contrast observed in biological samples is that the intensity variation is mainly due to the absorption of water [21]. With the additional spectroscopic information, this assumption can now be tested. In Fig. 8(a),

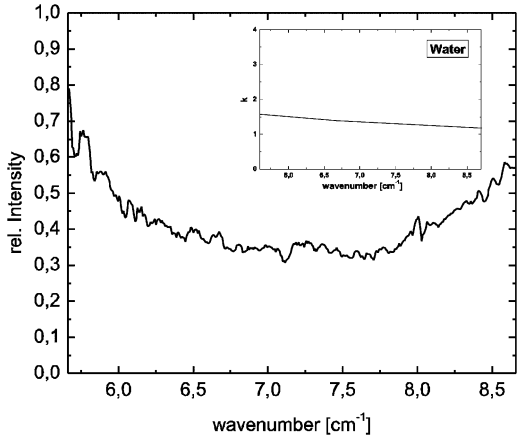

Fig. 8. THz near-field transmission spectrum recorded at a darker area of Fig. 7. The spectrum is normalized to the signal of the bare substrate. The image contrast is mainly due to the absorption, but cannot be explained by the absorption of water alone (see inset).

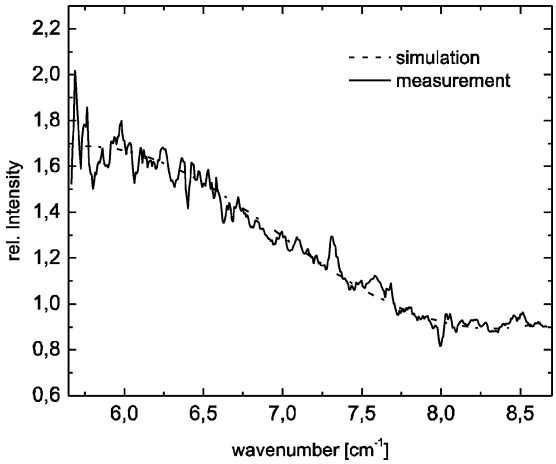

Fig. 10. THz-near-field spectrum recorded at a darker part of Fig. 9. The spectrum is normalized to the signal of the bare substrate. The simulation is for a layer system: 200 μm layer with $n = 1.55$ and no absorption on Si. Here, the image contrast is pure phase contrast.

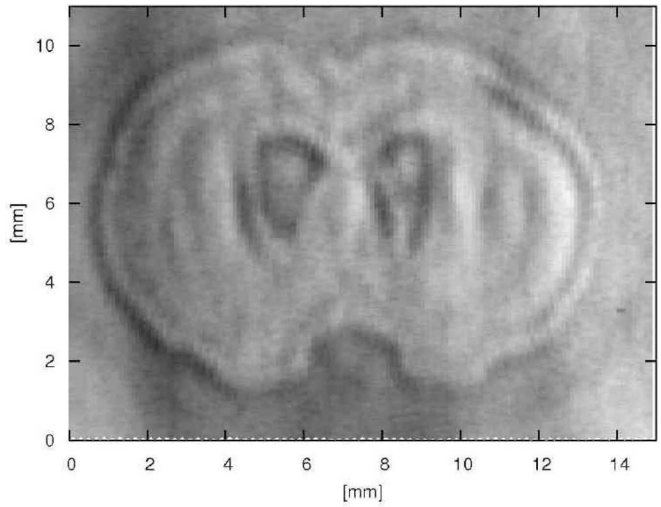

Fig. 9. THz-near-field image of a 200-μm-thick slice from a rat brain embedded in wax recorded at 220 GHz.

spectrum recorded at a subwavelength spot focused at a darker area of Fig. 7 is displayed. A pure water layer of the same thickness as the leaf would give a thousand times larger absorption, and one would expect that over the whole frequency range, the transmission slightly decreases toward lower frequencies (see inset). The absorption of water alone cannot explain the observed rise toward lower frequencies. There must be additional excitations at higher frequencies or an additional phase shift due to the different refractive index of the leaf compared to silicon.

As an example of a water-free sample, we have chosen a thin slice from a rat brain embedded in wax by a standard procedure (Fig. 9). The 200-μm-thick slice was directly prepared on a 150-μm-thick Si wafer. The overall transmission here is much higher, and surprisingly same areas appear even brighter than the bare substrate. Moreover, in the normalized near-field transmission spectrum, values well above 100% can be observed (Fig. 10). In addition to the experimental spectrum, a simulation is shown. In this modeling, the transmission through a layer system air/Si/rat brain 200 μm thick with n as a fit parameter and no absorption/air was calculated. For $n = 1.55$, a nearly perfect agreement between simulation and measurement was obtained. In this case, the observed image contrast is a pure phase contrast. In combination with the fit procedure, we were able to detect the differences in the refractive index of about 1%. Keeping in mind that the refractive index for all materials is much higher in the THz range than that in the visible, it is evident that THz near-field spectroscopy can be advanced to a powerful tool in life science.

VI. Conclusion

Backward wave oscillators as tunable continuous wave (cw)-sources are ideally suited for the different types of micro-spectroscopy in the THz range. With solid immersion lenses, an enhancement of the spatial resolution by a factor of n, the refractive index of the lens material is easily possible without loss of intensity and without a complicated probe–sample distance control. For applications in which a high dynamic range is more important than a very high spatial resolution, this method is a simple and very attractive alternative to real near-field techniques. Nevertheless, one has to be aware that in micro-spectroscopic applications, the resolution of a SIL system depends on the wavelength.

Although in an aperture SNOM, the achievable resolution and the decay of the evanescent field behind the pinhole are independent from the used wavelength; in practice, compared to the other two techniques, this method has several disadvantages. The intensity decreases with r^6 so that at higher resolution, the dynamic range is very limited and one needs a very accurate distance control. By using copper as an aperture material, the pinhole cannot be thinner than 10 μm; otherwise, due to the large skin depth in the THz range, more light will shine through the foil than through the pinhole. In practice, this leads to a very sharp decay of the near-field signal behind the pinhole.

The scattering-type SNOM with a photoinduced aperture is the most promising method to combine a high spatial resolution with a high dynamic range and the capability to record transmission spectra. Here, the resolution is freely adjustable by optics, and therefore, it is always possible to find a good compromise between resolution and dynamic range. With this instrument, it is possible to record the transmission spectra on subwavelength spot sizes without a complex probe–sample distance control and with nearly no restrictions as far as the samples under investigation are concerned. The shown biological examples demonstrate how useful the additional spectroscopic information is for the interpretation of the observed image contrast.

REFERENCES

[1] M. Labardi, P. G. Gucciardi, and M. Allegrini, *Near-Field Optical Microscopy*. Bologna, Italy: Compositori, 2000.

[2] B. T. Rosner and D. W. Van Der Weide, "High frequency near-field microscopy," *Rev. Sci. Instrum.*, vol. 73, pp. 2505–2525, Jul. 2002.

[3] D. Mittleman, Ed., *Sensing With Terahertz Radiation*. Berlin, Germany: Springer, 2002.

[4] O. Mitrofanov, M. Lee, J. W. P. Hsu, L. N. Pfeiffer, K. W. West, and J. D. Wynn, "Terahertz pulse propagation through small apertures," *Appl. Phys. Lett.*, vol. 79, pp. 907–909, Aug. 2002.

[5] J. Faist, F. Capasso, D. L. Sivco, C. Sirtori, A. L. Hutchinson, and A. Y. Cho, "Quantum cascade laser," *Science*, vol. 264, pp. 553–556, Apr. 1994.

[6] C. Kremser, W. Heiss, K. Unterrainer, E. Gornik, E. E. Haller, and W. K. Hansen, "Stimulated emission from p-Ge due to transitions between light-hole Landau levels and excited stated of shallow impurities," *Appl. Phys. Lett.*, vol. 60, pp. 1785–1787, Feb. 1992.

[7] G. Kozlov and A. Volkov, "Coherent source submillimeter wave spectroscopy," in *Millimeter and Submillimeter Wave Spectroscopy in Solids*, G. Grüner, Ed. Berlin, Germany: Springer, 1998, ch. 3, pp. 51–109.

[8] S. M. Mansfield and G. S. Kino, "Solid immersion microscope," *Appl. Phys. Lett.*, vol. 57, pp. 2615–2616, Dec. 1990.

[9] A. Pimenov and A. Loidl, "Focusing of millimetre-wave radiation beyond the Abbe barrier," *Appl. Phys. Lett.*, vol. 83, pp. 4122–4124, Nov. 2003.

[10] B. Gompf, M. Gerull, T. Müller, and M. Dressel, "THz-microspectroscopy with backward-wave oscillators," *Infrared Phys. Technol.*, vol. 49, pp. 128–132, 2006.

[11] E. A. Ash and G. Nicholls, "Super-resolution aperture scanning microsope," *Nature*, vol. 237, pp. 510–518, 1972.

[12] H. A. Bethe, "Theory of diffraction by small holes," *Phys. Rev.*, vol. 66, pp. 163–182, Oct. 1944.

[13] C. J. Bouwkamp, "On Bethe's theory of diffraction by small holes," *Philips Res. Rep.*, vol. 5, pp. 321–332, 1950.

[14] S. Mair, B. Gompf, and M. Dressel, "Spatial and spectral behavior of the optical near field studied by a terahertz near-field spectrometer," *Appl. Phys. Lett.*, vol. 84, pp. 1219–1221, Feb. 2004.

[15] A. Roberts, "Near-zone fields behind circular apertures in thick, perfectly conducting screens," *J. Appl. Phys.*, vol. 65, pp. 2896–2899, Apr. 1989.

[16] M. A. Ordal, R. J. Bell, R. W. Alexander, L. L. Long, and M. R. Querry, "Optical properties of fourteen metals in the infrared and far infrared: Al, Co, Cu, Au, Fe, Pb, Mo. Ni, Pd, Pt, Ag, Ti, V, and W," *Appl. Opt.*, vol. 24, no. 24, pp. 4493–4499, 1985.

[17] H.-T. Chen, R. Kersting, and G. C. Cho, "THz imaging with nanometer resolution," *Appl. Phys. Lett.*, vol. 83, pp. 3009–3011, Oct. 2003.

[18] D. V. Palanker, G. M. H. Knippels, T. I. S. Smith, and H. A. Schwettman, "Fast IR imaging with sub-wavelength resolution using a transient near-field probe," *Nucl. Instrum. Methods Phys. Res. B*, vol. 144, pp. 240–245, Sep. 1998.

[19] Q. Chen, Z. Jiang, G. X. Xu, and X. C. Zhang, "Near-field terahertz imaging with a dynamic aperture," *Opt. Lett.*, vol. 25, pp. 1122–1124, Aug. 2000.

[20] B. Gompf, N. Gebert, H. Heer, and M. Dressel, "Polarization contrast terahertz near-field imaging of anisotropic conductors," *Appl. Phys. Lett.*, vol. 90, pp. 082104-1–082104-3, Feb. 2007.

[21] S. Hadjiiloucas, L. S. Jaratzas, and J. W. Bowen, "Measurements of leaf water content using terahertz radiation," *IEEE Trans. Microw. Theory Tech.*, vol. 47, no. 2, pp. 142–149, Feb. 1999.

Bruno Gompf received the Sc.D. degree from the Universität Tübingen, Tübingen, Germany, in 1990.

He has been with the Universität Stuttgart, Stuttgart, Germany, where he currently has a permanent position. He has been engaged in various fields like scanning tunneling microscopy and sonoluminescence. His current research interests include organic semiconductors, ultrathin metal films, and terahertz-near-field techniques.

Martin Dressel received the Sc.D. degree from the Universität Göttingen, Göttingen, Germany, in 1989.

He was a Postdoctoral Research Fellow in applied laser science at the Universität Göttingen . He has also been with the University of British Columbia, Vancouver, BC; the University of California, Los Angeles, CA; the Technical Universität Darmstadt, Darmstadt, Germany; and the Center of Electronic Correlations and Magnetism at the Universität Augsburg, Augsburg, Germany. He is currently the Head of the Physikalischess Institut, Universität Stuttgart, Stuttgart, Germany. His current research interests include the electronic and magnetic properties of low-dimensional and correlated electron systems. His expertise includes microwave and infrared experiments on conductors and superconductors, and also nanoparticles and biomolecules. During the last ten years, he had established a worldwide-recognized laboratory for terahertz spectroscopy of solids.